Progress In Electromagnetics Research C, Vol. 42, 67–82, 2013

FAST SYNTHESIS OF LARGE PLANAR ARRAYS USING ACTIVE ELEMENT PATTERN METHOD AND FINE-GRAINED PARALLEL MICRO-GENETIC ALGORITHM

Ling-Lu Chen[1], Cheng Liao[1, *], Lei Chang[1], Hai-Jing Zhou[2], and Han-Yu Li[2]

[1]Institute of Electromagnetics, Southwest Jiaotong University, Chengdu, Sichuan 610031, China

[2]Institute of Applied Physics and Computational Mathematics, Beijing 100094, China

Abstract—A radiation pattern synthesis technique for large planar arrays with active element pattern (AEP) method and fine-grained parallel micro-genetic algorithm (FGPMGA) is presented. Based on the AEP method, the mutual coupling between array elements can be taken into account. Analysis problems of large rectangular and triangular grid planar arrays are divided into small linear array problems. And for a multiple concentric circular ring array, we only need to obtain one-sixth of all AEPs. So computational cost is greatly reduced. Large planar arrays with low side lobe level (SLL) can be achieved via optimizing the excitation amplitudes and phases. In order to reduce the global optimization time, the FGPMGA is used. This technique is applied to design 256-element rectangular grid, 200-element triangular grid and 4-circle 60-element concentric circular ring E-shaped patch antenna arrays. The radiation patterns calculated by the AEP method show good agreements with those by using CST Microwave Studio.

1. INTRODUCTION

Planar antenna arrays for mobile, remote sensing, satellite and radar communications systems can provide a good control of the radiation patterns. Typically, the elements of planar arrays are arranged in a rectangular, triangular grid or concentric circular ring. The performance of these systems is closely related with the antenna

Received 20 May 2013, Accepted 9 July 2013, Scheduled 17 July 2013

* Corresponding author: Cheng Liao (c.liao@swjtu.edu.cn).

array design. To gain high performance of the planar array, many synthesis methods that permit the calculation of the array excitation distribution are applied [1–10]. In [1], a method based on invasive weed optimization (IWO) algorithm and iterative Fourier technique (IFT) was proposed for the synthesis of large planar thinned arrays. Recently, global optimization algorithms have shown great potential in the solution of planar array synthesis problems, such as genetic algorithm (GA) [2–4], particle swarm optimization [5, 6], differential evolution strategy (DES) [7, 8], and ant colony optimization (ACO) [9]. In [10], a PGAPack parallel GA was used for the synthesis of planar phased-array antennas that can take a significantly greater amount of time to converge to the desired solution. However, these approaches all neglect the mutual coupling effects.

Full-wave electromagnetic simulations based on the finite-difference time-domain (FDTD) method [11, 12], finite element method (FEM) [13–15] and method of moment (MoM) [16–18] are applied to analyze the mutual coupling between antenna arrays. However, the calculation of most planar array antennas requires extremely long computation time, which makes it impossible to obtain the optimal excitation amplitudes and phases of array elements. Due to the computer memory limitations, full-wave methods are difficult to simulate the whole planar arrays, when the number of array elements is large.

Active element pattern (AEP) method which can rigorously include the effects of mutual coupling is an effective way to compute the far-field patterns of a fully excited array [19, 20]. The AEP is defined as the antenna pattern of a single excited element in the array, and all other elements terminated in matched loads. The AEP of each element is different from each other. The difference is mainly due to the different relative position of each element and mutual couplings between elements. In [21], AEP method is used to design linear microstrip arrays with taylor synthesis method. The AEP method has been applied for planar antenna array with asymmetrical elements [22]. For a circular array, array beamforming is achieved based on the AEP method and GA [23]. The AEP method has been widely used for analyzing conformal antenna arrays [24–27]. At present, the AEP method has not been applied to the triangular grid planar array and multiple concentric circular ring array.

In this paper, the AEP method is used to calculate the patterns of rectangular grid, triangular grid and multiple concentric circular ring E-shaped patch antenna arrays. The AEPs are calculated by CST Microwave Studio. Through optimizing excitation amplitudes or phases based on the fine-grained parallel micro-genetic algorithm

(FGPMGA), the desired radiation patterns are obtained. Our research shows that the FGPMGA significantly outperforms micro-genetic algorithm (MGA), in terms of both the convergence rate and exploration ability [28].

This paper is organized as follows. Section 2 describes the FGPMGA, a linear array pattern synthesis with low side lobe and a wide null is provided to demonstrate the advantages of FGPMGA. Section 3 gives the formulations of AEP method, and the correctness of this method is validated by using CST Microwave Studio. In Section 4 the 256-element rectangular grid, 200-element triangular grid and 4-circle 60-element concentric circular ring E-shaped patch antenna arrays are optimized by FGPMGA. Conclusions are given in Section 5.

2. FINE-GRAINED PARALLEL MICRO-GENETIC ALGORITHM

The fine-grained parallel model is also called neighborhood model. Each processor is allocated only one individual and selects parents for recombination from local neighborhood by considering neighbors at different distances. For the FGPMGA, a 4-n neighborhood is used, as shown in Fig. 1. In this case, each node represents a single individual. The FGPMGA is implemented using C++ on a message passing interface (MPI) environment.

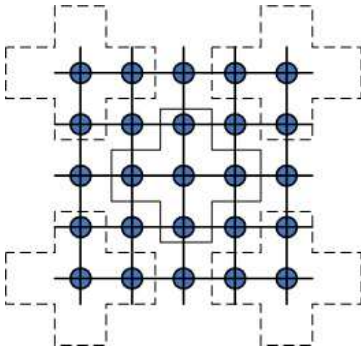

Figure 1. The FGPMGA architecture.

In each neighborhood, different crossover and mutation probability, as well as different methods of mutation and crossover. The procedure of the FGPMGA is described in [28].

A linear array with $2N$ elements is symmetrically placed on the x-axis, and the array factor for nonuniform excitation amplitude and

uniform excitation phase can be written as

$$AF(I,\theta) = 2\sum_{n=1}^{N} I_n \cos\left[\left(\frac{2n-1}{2}\right) kd\sin\theta\right] \tag{1}$$

where, d ($d = 0.5\lambda$) is the separation between the elements; I_n is the excitation amplitude of nth element; k is the propagation constant; θ is the elevation angle.

To validate the effectiveness of FGPMGA, we synthesize a 32-element ($N = 16$) linear array with a wide null located at $45^\circ \sim 50^\circ$. 5 independent runs of the FGPMGA are repeated. The desired sidelobe level $DSLL = -20\,\text{dB}$ and the null depth level $DNULL = -40\,\text{dB}$ [29]. The population size and fitness function are the same settings as in [29].

Figure 2 shows the optimal excitation amplitudes optimized by FGPMGA. The average convergence rate of the parallel algorithm is shown in Fig. 3. The normalized radiation pattern is given in Fig. 4. Table 1 shows the comparative results obtained by FGPMGA and improved differential evolution (IDE) algorithm proposed in [29]. It can be seen that the SLL and null depth level found by FGPMGA are

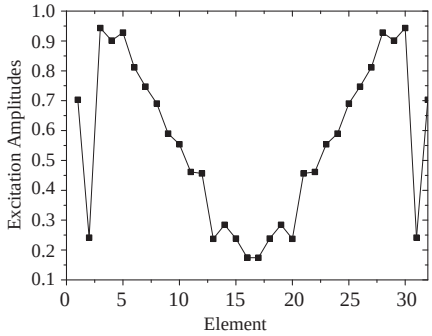

Figure 2. Excitation amplitudes by FGPMGA for the linear array.

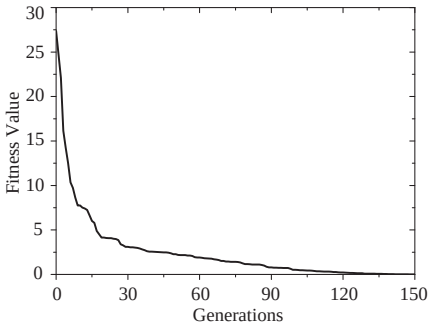

Figure 3. Average convergence rate for the linear array.

Table 1. Comparisons of the optimized results for FGPMGA and algorithm proposed in [29].

	SLL	Null depth level	Number of iterations
FGPMGA	$-31.64\,\text{dB}$	less than $-50\,\text{dB}$	150
algorithm in [29]	$-22\,\text{dB}$	less than $-40\,\text{dB}$	about 170

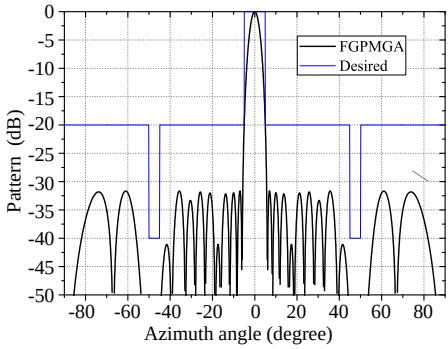

Figure 4. Radiation pattern for 32-element symmetric array.

smaller than those obtained by the IDE, as well as FGPMGA needs less number of iterations.

3. ACTIVE ELEMENT PATTERN METHOD FOR PLANAR ANTENNA ARRAY

3.1. Rectangular Grid Planar Array

We construct a uniform 256-element rectangular grid planar E-shaped patch antenna array, as shown in Fig. 5. The distances between elements in the x and y direction are 45 mm ($0.79\,\lambda$ at the operating frequency 5.25 GHz). The E-shaped patch antenna element was optimized in [30]. We change the size of ground to 40 mm $\times$ 40 mm. As the excitation phases are 0, the radiation pattern of xz-plane can be expressed using active element patterns as

$$E(\theta, \varphi = 0) = \sum_{m=1}^{N_x} \sum_{n=1}^{N_y} I_{mn} E_{mn}(\theta, \varphi = 0) e^{jkmd_x \sin\theta} \tag{2}$$

and yz-plane is

$$E(\theta, \varphi = 90^\circ) = \sum_{m=1}^{N_x} \sum_{n=1}^{N_y} I_{mn} E_{mn}(\theta, \varphi = 90^\circ) e^{jknd_y \sin\theta} \tag{3}$$

where, $d_x = d_y = 45$ mm are the inter-element spacings; $N_x = N_y = 16$ are the number of elements in x and y directions; k is the free-space propagation constant; θ denotes the azimuth angle; I_{mn} are the excitation amplitudes for $m = 1, \ldots, N_x$ and $n = 1, \ldots, N_y$; E_{mn} are the active element patterns for $m = 1, \ldots, N_x$ and $n = 1, \ldots, N_y$.

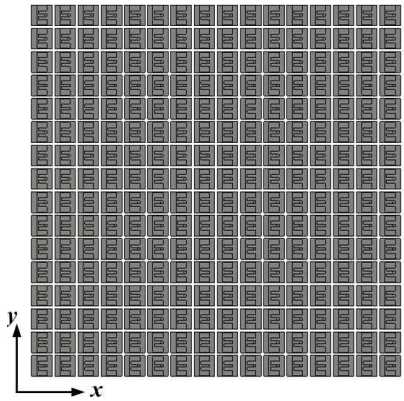

Figure 5. Configuration of the 256-element rectangular grid planar array.

The patterns of the principal planes can be deduced from two small N_s-element (N_s is odd and less than N_x, N_y) linear arrays. The procedure can be described as follows [31]:

1. Calculate the AEPs of N_s-element linear antenna arrays arranged along both the x and y axis. The AEPs of i-th element in x and y axis are set as $E_{N_s,i}(\theta, \varphi = 0)$ and $E_{N_s,i}(\theta, \varphi = 90^\circ)$ respectively.

2. In x-axis, the m-th AEP $E_{N_x,m}(\theta, \varphi = 0)$ of N_x-element linear array is,

$$\begin{aligned} &E_{N_x,m}(\theta,0)|_{m=1,\ldots,\frac{N_s+1}{2}-1} = E_{N_s,m}(\theta,0)|_{m=1,\ldots,\frac{N_s+1}{2}-1} \\ &E_{N_x,m}(\theta,0)|_{m=\frac{N_s+1}{2},\ldots,N_x-\frac{N_s+1}{2}+1} = E_{N_s,m}(\theta,0)|_{m=\frac{N_s+1}{2}} \\ &E_{N_x,m}(\theta,0)|_{m=N_x-\frac{N_s+1}{2}+2,\ldots,N_x} = E_{N_s,m}(\theta,0)|_{m=\frac{N_s+1}{2}+1,\ldots,N_s} \end{aligned} \tag{4}$$

In y-axis, the n-th AEP $E_{N_y,n}(\theta, \varphi = 90^\circ)$ of N_y-element linear array is,

$$\begin{aligned} &E_{N_y,n}(\theta,90^\circ)|_{n=1,\ldots,\frac{N_s+1}{2}-1} = E_{N_s,n}(\theta,90^\circ)|_{n=1,\ldots,\frac{N_s+1}{2}-1} \\ &E_{N_y,n}(\theta,90^\circ)|_{n=\frac{N_s+1}{2},\ldots,N_y-\frac{N_s+1}{2}+1} = E_{N_s,n}(\theta,90^\circ)|_{n=\frac{N_s+1}{2}} \\ &E_{N_y,n}(\theta,90^\circ)|_{n=N_y-\frac{N_s+1}{2}+2,\ldots,N_y} = E_{N_s,n}(\theta,90^\circ)|_{n=\frac{N_s+1}{2}+1,\ldots,N_s} \end{aligned} \tag{5}$$

3. When $\varphi = 0$, the AEPs of the planar array in L-th line are

$$E_{N_x,L,m}(\theta,0)|_{m=1,\ldots,N_x}^{L=2,\ldots,N_y} = E_{N_x,m}(\theta,0)|_{m=1,\ldots,N_x} \tag{6}$$

when $\varphi = 90^\circ$, the AEPs of the planar array in C-th column are,

$$E_{N_y,C,n}(\theta,90^\circ)|_{n=1,\ldots,N_y}^{C=2,\ldots,N_x} = E_{N_y,n}(\theta,0)|_{n=1,\ldots,N_y} \tag{7}$$

4. Using Eqs. (2) and (3), we can obtain the radiation patterns in the principal planes.

The amplitude I_{mn} is set as 1. As shown in Fig. 6, for $N_s = 5$, the radiation patterns of the 256-element rectangular grid planar array in the xz and yz planes computing using Eqs. (2) and (3) are compared to the patterns full-wave simulated by CST. We can see that the results computed using AEP method are consistent with the CST simulations when the planar array is fully excited. The maximum gain is 32.9 dBi.

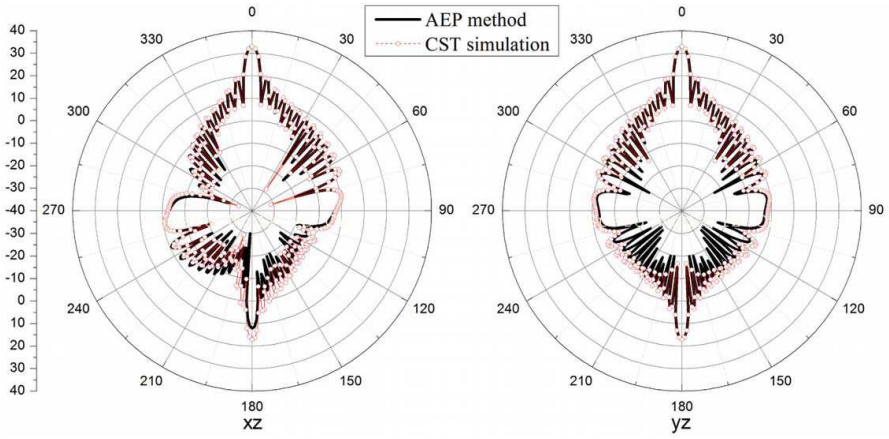

Figure 6. Radiation patterns of the 256-element rectangular grid planar array.

3.2. Triangular Grid Planar Array

A uniform triangular grid planar array composed of 200 E-shaped patch antennas (see Fig. 7). The excitation phases are set as 0. So the far field of xz-plane is given by

$$E(\theta, 0) = \left(1 + e^{jkd_x \sin\theta}\right) \sum_{m=1}^{N_x} \sum_{n=1}^{N_y} I_{mn} E_{mn}(\theta, 0) e^{jk2md_x \sin\theta} \tag{8}$$

and radiation pattern of yz-plane is expressed as

$$E(\theta, 90^\circ) = \left(1 + e^{jkd_y \sin\theta}\right) \sum_{m=1}^{N_x} \sum_{n=1}^{N_y} I_{mn} E_{mn}(\theta, 90^\circ) e^{jk2nd_y \sin\theta} \tag{9}$$

where, $d_x = d_y = 45\,\text{mm}$, $N_x = N_y = 10$, and k is the free-space propagation constant; θ, E_{mn} and I_{mn} are the same meanings as in Eqs. (2) and (3).

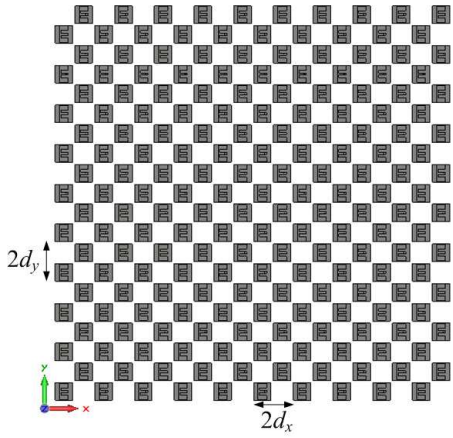

Figure 7. Configuration of the 200-element triangular grid planar array.

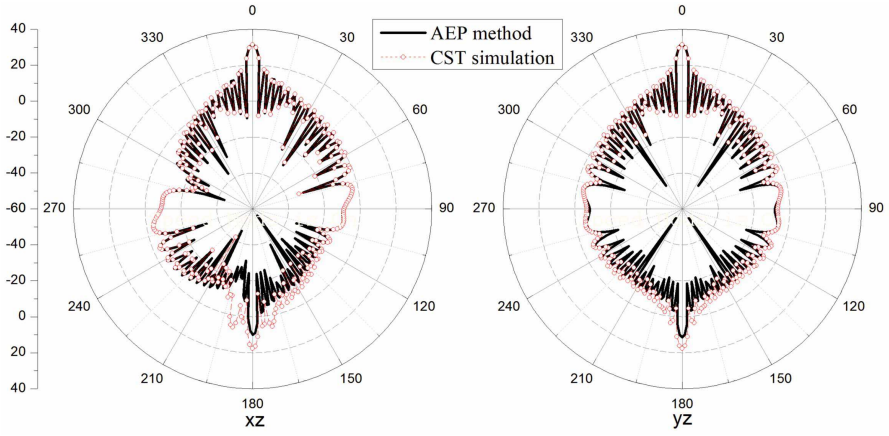

Figure 8. Radiation patterns of the 200-element triangular grid planar array.

The analysis problem of triangular grid planar array can also be divided into small linear array problems just like rectangular grid planar array. Using two 5-element linear arrays, we can obtain all AEPs of this array. All excitation amplitudes are the same. From Eqs. (8) and (9), the radiation patterns of the principal planes have been computed, and the results given by the AEP method and CST simulation are shown in Fig. 8. It is shown that the results are in good

agreement. The maximum gain is 31.3 dBi.

3.3. Multiple Concentric Circular Ring Array

A concentric circular ring E-shaped patch antenna array with four rings is shown in Fig. 9. The number of elements in the ring is 6, 12, 18, and 24, respectively. The far field pattern is given by

$$\begin{aligned} E(\theta,\varphi) \;=\; & \sum_{a=1}^{6} I_1 E_a(\theta,\varphi) e^{j(kr_1 \sin\theta\cos(\varphi-\varphi_a)+\phi_1)} \\ & + \sum_{b=1}^{12} I_2 E_b(\theta,\varphi) e^{j(kr_2 \sin\theta\cos(\varphi-\varphi_b)+\phi_2)} \\ & + \sum_{c=1}^{18} I_3 E_c(\theta,\varphi) e^{j(kr_3 \sin\theta\cos(\varphi-\varphi_c)+\phi_3)} \\ & + \sum_{d=1}^{24} I_4 E_d(\theta,\varphi) e^{j(kr_4 \sin\theta\cos(\varphi-\varphi_d)+\phi_4)} \end{aligned} \tag{10}$$

where, $\varphi_a = \frac{2\pi(a-1)}{6}$, $\varphi_b = \frac{2\pi(b-1)}{12}$, $\varphi_c = \frac{2\pi(c-1)}{18}$, $\varphi_d = \frac{2\pi(d-1)}{24}$; I_1, I_2, I_3, I_4 are the excitation amplitudes; ϕ_1, ϕ_2, ϕ_3, ϕ_4 are the excitation phases; r_1, r_2, r_3, r_4 are the radii of the four rings, and $r_1 = 55\,\text{mm}$ (0.96λ), $r_2 = 110\,\text{mm}$, $r_3 = 165\,\text{mm}$, $r_4 = 220\,\text{mm}$.

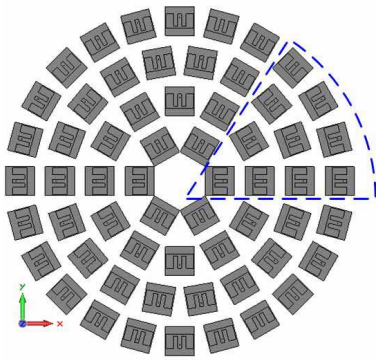

Figure 9. Configuration of the 60-element concentric circular ring array.

We only need to calculate the AEPs of 10 elements in the dashed box (see Fig. 9). The others can be given by

$$E_m(\theta,\varphi) = E_i(\theta,\varphi-\phi_m)\, e^{j\phi_m} \tag{11}$$

where, $E_m(\theta, \varphi)$ is the m-th unknown AEP, $E_i(\theta, \phi_m)$ is the i-th known AEP, and ϕ_m is the included angle between the m-th unknown element and i-th known element.

An analysis is given of the 4-ring array with excitation amplitudes equal to 1 and phases equal to 0. The radiation patterns are obtained from the Eq. (10). Fig. 10 shows the far field patterns by using the AEP method and CST simulation. Note that the results of the two methods are in good agreement.

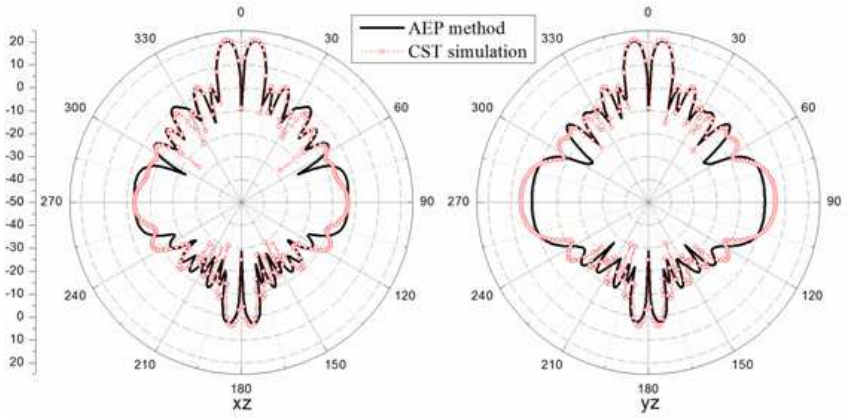

Figure 10. Radiation patterns of the 60-element concentric circular ring array.

4. OPTIMIZATION RESULTS OF PLANAR ANTENNA ARRAYS

The planar E-shaped patch antenna arrays are optimized by the FGPMGA on the Dawning 5000 computer system (belong to Institute of Applied Physics and Computational Mathematics).

4.1. Optimization of Rectangular Grid Planar Array

In the first example, a rectangular grid planar antenna array as shown in Fig. 5 is optimized. The excitation phases are set as 0. The optimized parameters are the excitation amplitude of each element and the objective function is to generate the minimum side lobe level (SLL) and keep the maximum gain same as the patterns in Section 2.1. The fitness function is given by

$$F(\bar{x}) = w_1 \cdot SLL + w_2 \cdot (Gain_{\max} - 32.9 \text{ dBi}) \tag{12}$$

where, $\bar{x} = I_{1,1}, \ldots, I_{16,16}$; SLL indicates side lobe level, and $Gain_{\max}$ is the maximum gain of planar array; w_1 and w_2 are weight factors. The population size is set to 400 and the total number of iterations is 2000.

Figure 11 shows the optimized patterns. It can be seen that the SLL of xz-plane is reduced from -13.25 dB to -20.53 dB, the SLL of yz-plane is reduced from -13.35 dB to -18.25 dB, and the maximum gain is 31.9 dBi. The optimization time by using the FGPMGA with 400 processors is about two hours in contrast to five days by using MGA on the personal computer.

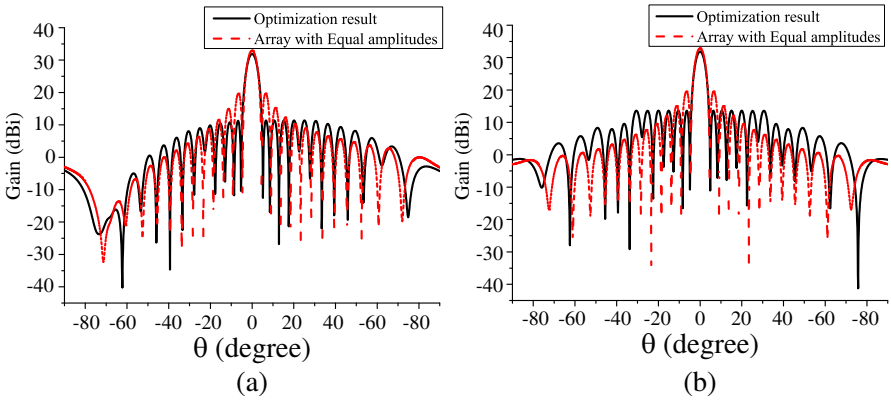

Figure 11. Optimization radiation patterns of rectangular grid planar array. (a) xz-plane. (b) yz-plane.

4.2. Optimization of Triangular Grid Planar Array

In this example, amplitude-only pattern synthesis is used for triangular grid planar array (see Fig. 7). Our objectives are to meet the minimum SLL, and the same maximum gain as the array with equal amplitudes in Section 2.2. The fitness function is given by

$$F(\bar{x}) = w_1 \cdot SLL + w_2 \cdot (Gain_{\max} - 31.3 \text{ dBi}) \tag{13}$$

where, $\bar{x} = I_{1,1}, \ldots, I_{10,10}$; SLL, $Gain_{\max}$, w_1 and w_2 are the same meanings as in Eq. (12). The following FGPMGA parameter values are selected: the number of individuals and generations is 400 and 2000, respectively.

Shown in Fig. 12 is the optimized radiation patterns of the principal planes. It is found that the SLLs of xz-plane and yz-plane obtained by the FGPMGA are -15.94 dB and -16.54 dB, respectively,

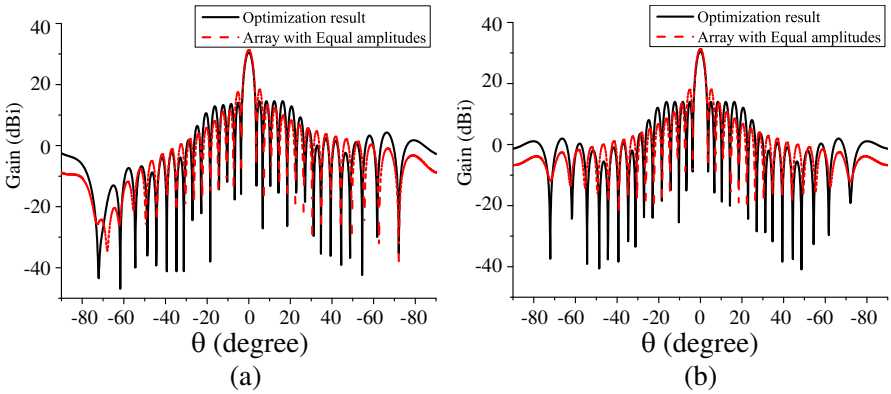

Figure 12. Optimization radiation patterns of triangular grid planar array. (a) xz-plane. (b) yz-plane.

in contrast to −12.98 dB and −13.28 dB of the array with equal amplitudes. The maximum gain is 30.5 dBi. The FGPMGA with 400 processors only needs 1.3 hours for computing, while MGA on the personal computer needs about three days.

4.3. Optimization of Multiple Concentric Circular Ring Array

In the last example, amplitude-phase pattern synthesis is used to make the power patterns of 4-ring array (see Fig. 9) be well matching with the desired patterns. The objective function is defined as

$$F(\bar{x}) = \omega_1 \sum_{\theta} \text{abs}\left|\frac{E_{main}(\theta,\varphi)}{E_{\max}} - 1\right| + \omega_2 \sum_{\theta}\left(\frac{E_{else}(\theta,\varphi)}{E_{\max}}\right) \quad (14)$$

where, $\bar{x} = I_1, I_2, I_3, I_4, \phi_1, \phi_2, \phi_3, \phi_4$, $0 \le I_i \le 1$, $0 \le \phi_i \le 2\pi$; $\omega_1 = 10$ and $\omega_2 = 1$ are the weight factors; $E_{\max}$ is the maximum radiation electric field; $E_{main}(\theta,\varphi)$ indicates the radiation electric field of main lobe, and $E_{else}(\theta,\varphi)$ indicates the radiation electric field in other regions. In the FGPMGA parameters, the initial population is set to 100, and the maximum number of iterations is 200.

First, we aim to produce a conical beam covering the sector $5^\circ \le |\theta| \le 20^\circ$. The resulting beam patterns are shown in Fig. 13. The patterns of the principal planes are close to the desired pattern.

Next, a conical beam covering the sector $15^\circ \le |\theta| \le 30^\circ$ is generated. Fig. 14 shows the optimized results. It can be seen that the resulting beam pattern closely resembles to the desired pattern.

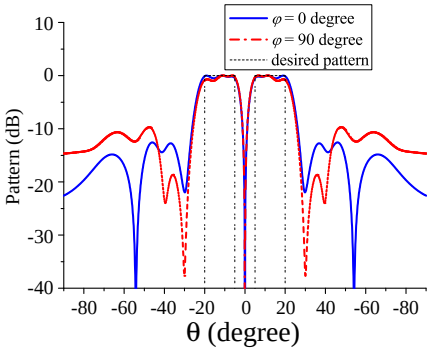

Figure 13. Radiation patterns optimized for covering the sector $5^\circ \leq |\theta| \leq 20^\circ$.

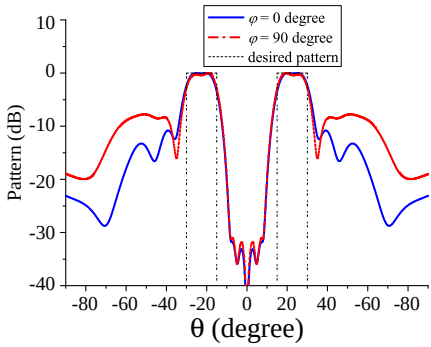

Figure 14. Radiation patterns optimized for covering the sector $15^\circ \leq |\theta| \leq 30^\circ$.

5. CONCLUSION

In this paper, we propose a technique based on AEP method and FGPMGA for large planar antenna array design. The AEP algorithm is used for computing the far field patterns of rectangular, triangular grid and multiple concentric circular ring planar arrays. The patterns obtained by the AEP method and CST Microwave Studio are in good agreements. The studies show that the AEP method is valid. For the three types of planar array synthesis as design examples, the FGPMGA achieves satisfactory results for planar arrays with many design variables to be determined, and effectively reduces the optimization time.

ACKNOWLEDGMENT

This work was supported by the National Basic Research Program of China (973 Program, Grant No. 2013CB328904), the NSAF of China (Grant No. 11076022), and the Research Fund of Key Laboratory of HPM Technology (2012-LHWJJ.006).

REFERENCES

1. Wang, X. K., Y. C. Jiao, L. Liu, and Y. Y. Tan, "Synthesis of large planar thinned arrays using IWO-IFT algorithm," *Progress In Electromagnetics Research*, Vol. 136, 29–42, 2013.
2. Zhou, H. J., B. H. Sun, J. F. Li, and Q. Z. Liu, "Efficient optimization and realization of a shaped-beam planar array

for very large array application," *Progress In Electromagnetics Research*, Vol. 89, 1–10, 2009.

3. Bianchi, D., S. Genovesi, and A. Monorchio, "Constrained pareto optimization of wide band and steerable concentric ring arrays," *IEEE Transactions on Antennas and Propagation*, Vol. 60, No. 7, 3195–3204, 2012.
4. Son, S. H., S. I. Jeon, C. J. Kim, and W. Hwang, "GA-based design of multi-ring arrays with omnidirectional conical beam pattern," *IEEE Transactions on Antennas and Propagation*, Vol. 58, No. 5, 1527–1535, 2010.
5. Wang, W. B., Q. Y. Feng, and D. Liu, "Synthesis of thinned linear and planar antenna arrays using binary PSO algorithm," *Progress In Electromagnetics Research*, Vol. 127, 371–378, 2012.
6. Lanza, M., J. R. Perez, and J. Basterrechea, "Synthesis of planar arrays using a modified particle swarm optimization algorithm by introducing a selection operator and elitism," *Progress In Electromagnetics Research*, Vol. 93, 145–160, 2009.
7. Mandal, A., H. Zafar, S. Das, and A. V. Vasilakos, "Efficient circular array synthesis with a memetic differential evolution algorithm," *Progress In Electromagnetics Research B*, Vol. 38, 367–385, 2012.
8. Zhang, L., Y. C. Jiao, Z. B. Weng, and F. S. Zhang, "Design of planar thinned arrays using a boolean differential evolution algorithm," *IET Microwaves, Antennas and Propagation*, Vol. 4, No. 12, 2172–2178, 2010.
9. Oliveri, G. and L. Poli, "Optimal sub-arraying of compromise planar arrays through an innovative ACO-weighted procedure," *Progress In Electromagnetics Research*, Vol. 109, 279–299, 2010.
10. Villegas, F. J., "Parallel genetic-algorithm optimization of shaped beam coverage areas using planar 2-D phased arrays," *IEEE Transactions on Antennas and Propagation*, Vol. 55, No. 6, 1745–1753, 2007.
11. Conceicao, R. C., M. O'Halloran, M. Glavin, and E. Jones, "Comparison of planar and circular antenna configurations for breast cancer detection using microwave imaging," *Progress In Electromagnetics Research*, Vol. 99, 1–20, 2009.
12. Guo, Y., X. L. Yang, W. H. Yu, and W. Y. Yin, "An effective simulation technique for large phased arrays using parallel FDTD method," *2012 IEEE International Symposium on Electromagnetic Compatibility, (EMC 2012)*, 103–107, 2012.
13. Alam, M. S., M. T. Islam, and N. Misran, "A novel

compact split ring slotted electromagnetic bandgap structure for microstrip patch antenna performance enhancement," *Progress In Electromagnetics Research*, Vol. 130, 389–409, 2012.

14. Islam, M. T. and M. S. Alam, "Compact EBG structure for alleviating mutual coupling between patch antenna array elements," *Progress In Electromagnetics Research*, Vol. 137, 425–438, 2013.
15. Casula, G. A., G. Mazzarella, and G. Montisci, "Design of shaped beam planar arrays of waveguide longitudinal slots," *International Journal of Antennas and Propagation*, Vol. 2013, 12, 2013.
16. Zhao, X. W., Y. Zhang, H. W. Zhang, D. G. Donoro, S. W. Ting, T. K. Sarkar, and C. H. Liang, "Parallel MoM-PO method with out-of-core technique for analysis of complex arrays on electrically large platforms," *Progress In Electromagnetics Research*, Vol. 108, 1–21, 2010.
17. Wang, W. T., S. X. Gong, Y. J. Zhang, F. T. Zha, J. Ling, and T. T. Wan, "Low RCS dipole array synthesis based on mom-pso hybrid algorithm," *Progress In Electromagnetics Research*, Vol. 94, 119–132, 2009.
18. Becker, O. and R. Shavit, "Efficient full-wave method of moments analysis and design methodology for radial line planar antennas," *IEEE Transactions on Antennas and Propagation*, Vol. 59, No. 6, 2294–2302, 2011.
19. Kim, J., J. So, W. Jang, and C. Cheon, "Gain estimation by convergence of active element pattern for E-plane notch phased array antenna," *Microwave and Optical Technology Letters*, Vol. 49, No. 5, 1047–1049, 2007.
20. Bai, Y. Y., S. Q. Xiao, M. C. Tang, Z. F. Ding, and B. Z. Wang, "Wide-angle scanning phased array with pattern reconfigurable elements," *IEEE Transactions on Antennas and Propagation*, Vol. 59, No. 11, 4071–4076, 2011.
21. He, Q. Q. and B. Z. Wang, "Design of microstrip array antenna by using active element pattern technique combining with taylor synthesis method," *Progress In Electromagnetics Research*, Vol. 80, 63–76, 2008.
22. Bhattacharyya, A. K., "Active element pattern symmetry for asymmetrical element arrays," *IEEE Antennas and Wireless Propagation Letters*, Vol. 6, 275–278, 2007.
23. Su, T. and H. Ling, "Array beamforming in the presence of a mounting tower using genetic algorithms," *IEEE Transactions on Antennas and Propagation*, Vol. 53, No. 6, 2011–2019, 2005.

24. Wang, Q. and Q. Q. He, "An arbitrary conformal array pattern synthesis method that include mutual coupling and platform effects," *Progress In Electromagnetics Research*, Vol. 110, 297–311, 2010.
25. Li, W. T., Y. Q. Hei, and X. W. Shi, "Pattern synthesis of conformal arrays by a modified particle swarm optimization," *Progress In Electromagnetics Research*, Vol. 117, 237–252, 2011.
26. Yang, X. S., H. Qian, B. Z. Wang, and S. Xiao, "Radiation pattern computation of pyramidal conformal antenna array with active-element pattern technique," *IEEE Antennas and Propagation Magazine*, Vol. 53, No. 1, 28–37, 2011.
27. Ouyang, J., X. Luo, J. Yang, K. Z. Zhang, J. Zhang, and F. Yang, "Analysis and synthesis of conformal conical surface linear phased array with volume surface integral equation plus AEP (active element pattern) and INSGA-II," *IET Microwaves, Antennas and Propagation*, Vol. 6, No. 11, 1277–1285, 2012.
28. Chang, L., H. J. Zhou, L. L. Chen, X. Z. Xiong, and C. Liao, "The fine-grained parallel micro-genetic algorithm and its application to broadband conical corrugated-horn antenna," *Progress In Electromagnetics Research*, Vol. 138, 599–611, 2013.
29. Li, R., L. Xu, X. W. Shi, N. Zhang, and Z. Q. Lv, "Improved differential evolution strategy for antenna array pattern synthesis problems," *Progress In Electromagnetics Research*, Vol. 113, 429–441, 2011.
30. Chang, L., C. Liao, W. B. Lin, L. L. Chen, and X. Zheng, "A hybrid method based on differential evolution and continuous ant colony optimization and its application on wideband antenna design," *Progress In Electromagnetics Research*, Vol. 122, 105–118, 2012.
31. Zhang, S., S. X. Gong, Y. Guan, and Q. Gong, "Extrapolative method in pattern calculation and synthesis of large plane arrays," *Chinese Journal of Computational Physics*, Vol. 28, No. 4, 554–560, 2011.